Author Manuscript

Author Manuscript

Author Manuscript

Author Manuscript

HHS Public Access

Author manuscript

*J Biomech*. Author manuscript; available in PMC 2016 October 15.

Published in final edited form as:

*J Biomech*. 2015 October 15; 48(13): 3634–3642. doi:10.1016/j.jbiomech.2015.08.011.

# Loading-induced Changes on Topographical Distributions of the Zonal Properties of Osteoarthritic Tibial Cartilage – A Study by Magnetic Resonance Imaging at Microscopic Resolution

**Ji Hyun Lee**[1], **Farid Badar**[1], **David Kahn**[1], **John Matyas**[2], **Xianggui Qu**[3], and **Yang Xia**[1,*]

[1]Department of Physics and Center for Biomedical Research, Oakland University, Rochester, MI 48309, USA

[2]Department of Comparative Biology and Experimental Medicine, Faculty of Veterinary Medicine, University of Calgary, Calgary, AB T2N 4N1, Canada

[3]Department of Mathematics and Statistics, Oakland University, Rochester, MI 48309, USA

## Abstract

The topographical distributions of the zonal properties of articular cartilage over the medial tibia from an experimental osteoarthritis (OA) model were evaluated as the function of external loading by microscopic Magnetic Resonance Imaging (μMRI). T2 relaxation times and cartilage thicknesses were measured at 17.6μm resolution from 118 specimens, which came from thirteen dogs (six 8-week and seven 12-week after surgery), with and without mechanical loading. In addition, bulk mechanical modulus was measured topographically from each tibia surface. The total thickness decreased significantly under the external loading, in which the relative thickness of the superficial zone (SZ) and the transitional zone (TZ) increased whereas the radial zones (RZs) decreased. In the bulk data, T2(55°) decreased significantly ($p<0.001$) at all OA-time-points, but T2(0°) decreased without significance ($p>0.05$) at 8-week. Complex relationships were found in the zonal tissue properties as a function of external loading with the progress of OA. T2 in the superficial zone changed more profoundly than the same properties in the radial zone as the function of external loading at all OA time-points. This study confirms that the OA affects the load-induced changes in the molecular distribution and structure of cartilage, which are both depth-dependent and topographically distributed. Such detailed knowledge of mechanobiological changes in specific tibial cartilage zones and locations with OA progress could improve the early detection of the subtle softening of cartilage that accompany pre-clinical stages of OA.

*Corresponding Author and Address: Yang Xia, Ph.D., Department of Physics, Oakland University, Rochester, Michigan 48309, USA, Phone: (248) 370-3420, Fax: (248) 370-3408, xia@oakland.edu.

Conflict of interest statement: The authors declare no conflicts of interests.

**Publisher's Disclaimer:** This is a PDF file of an unedited manuscript that has been accepted for publication. As a service to our customers we are providing this early version of the manuscript. The manuscript will undergo copyediting, typesetting, and review of the resulting proof before it is published in its final citable form. Please note that during the production process errors may be discovered which could affect the content, and all legal disclaimers that apply to the journal pertain.

Author Manuscript Author Manuscript Author Manuscript Author Manuscript

**Keywords**

Magnetic Resonance Image (MRI); Strain; Cartilage; T2 relaxation time; Osteoarthritis (OA); mechanical modulus

## 1. Introductions

Degeneration of cartilage is a hallmark of osteoarthritis (OA), which is the most common type of arthritis (Murphy L, 2008). Since articular cartilage is a load-bearing tissue (Alhadlaq and Xia, 2004, 2005; Brama et al., 2009a; Eckstein et al., 2002), compressive loading on cartilage can introduce some complex consequences (Chen et al., 2001), resulting in various changes in the molecular environment and ultrastructural network of the tissue (Lee et al., 2014a). Since the mechanical properties of cartilage are closely related to the degradation of cartilage, a sensitive technique for non-destructively detecting the structural, topographical, and functional changes in cartilage would be invaluable for the diagnostic monitoring of OA progression and for the efficacy evaluation of OA treatment.

MRI has been used extensively in cartilage imaging, including the parameters and protocols of T2 relaxation, T1rho relaxation, sodium MRI, and gadolinium-contrasted imaging (Fragonas et al., 1998; Xia, 1998; Xia and Elder, 2001). T2, the spin-spin relaxation time, reflects the dynamic motion of the water molecules in cartilage and is sensitive to the interactions of water with the macromolecules (mainly collagen fibers and proteoglycans), which monitors the integrity and anisotropy of the extracellular matrix (Xia, 1998). For example, T2 value was found to increase in OA cartilage, which reflects the loss of proteoglycan and softening of the tissue (Alhadlaq et al., 2004; Dunn et al., 2004; Jones et al.; Stahl et al., 2007). Correlation between T2 and the mechanical properties of cartilage were also established in both human and animals (Lee et al., 2014a; Nissi et al., 2007; Wayne et al., 2003).

Two major difficulties in cartilage imaging are its complex topographical variations and its strong depth-dependent properties. The topographical variations refer to the fact that all cartilage measurements (including biomechanical and biochemical properties of articular cartilage) are known to vary with different locations on the surface of a single joint (Alhadlaq and Xia, 2005; Alhadlaq et al., 2004; Brama et al., 2009b; Jurvelin et al., 2000; Lee et al., 2014a; Weiss et al., 1968; Xia, 2000; Xia et al., 2003). The depth-dependent (zonal) properties refer to the anisotropic and nonlinear profiles of many cartilage properties across its thin thickness (Alhadlaq and Xia, 2005; Alhadlaq et al., 2004; Lee et al., 2014a), which are caused largely by the spatial structure of the collagen matrix in cartilage from the superficial zone (SZ), to the transitional zone (TZ), to the radial zone (RZ). Since mechanical modulus in cartilage is depth-dependent, the responses to external loading in cartilage must also be depth-dependent (Alhadlaq and Xia, 2005; Alhadlaq et al., 2007; Alhadlaq et al., 2004; Xia et al., 2008). Consequently, the response of cartilage to external loading should be both topographically and disease dependent (Lee et al., 2014b), which implies the need of high resolution imaging in such study. Understanding that T2 is highly sensitive to the early progression of OA when the tissue is not compressed (Alhadlaq et al., 2004), we hypothesized in this project that the strain-dependency of the zonal properties of

Author Manuscript Author Manuscript Author Manuscript Author Manuscript

cartilage T2 could predict the biomechanical properties of degenerated cartilage. We aimed to investigate the loading-induced modifications to both topographical and depth-dependent properties of cartilage (tissue thickness and T2) in meniscus-covered and uncovered areas on the medial tibia of the canine knee at different OA time-points of the experimentally developed disease.

## 2. Materials and Methods

### 2.1. Cartilage specimens

With the approval of local institutional review committees, thirteen skeletally matured dogs underwent the anterior (cranial) cruciate ligament transection (ACLx) in one knee. The contralateral knees of all animals received no surgery. The dogs were sacrificed 8-week (6 dogs) and 12-week (7 dogs) post-surgery. As such, the OA-time points of the specimens were: 8X: the specimens from the 8-week post-surgical knees, 8C: the specimens from the 8-week contralateral knees, 12X: the specimens from the 12-week post-surgical knees, and 12C: specimens from the 12-week contralateral knees. (In addition, the data of 61 specimens from 14 healthy knees from the previous control study were also used in the compative analysis (Lee et al., 2014a).) From each medial tibial plateau, five rectangular specimens ($3.0\times2.5\times4\sim5\ mm^3$) were harvested (Lee et al., 2014a). All specimens were immersed in saline with 1 mM gadolinium (Magnevist, Berlex, NJ) at 4°C until imaging. The specimen was placed at room temperature (~20°C) for about 4 hours before μMRI. A total of 118 specimens from 26 medial tibias were imaged twice before and after loading, both times inside a 4.34-mm glass tube (Alhadlaq and Xia, 2004; Lee et al., 2014a). The tissue loading was carried out manually in a custom-made non-magnetic loading device (Alhadlaq and Xia, 2004; Lee et al., 2014a).

### 2.2. Biomechanical protocols

Before harvesting the individual specimens from the tibia, a single step indentation experiment was performed on all thirteen intact joint surfaces. An approximately 10-grams load was applied to the tissue surface by a 5 mm diameter round-tip indenter that was attached to the actuator of an EnduraTec ELF 3200 system (Bose, Eden Prairie, MN). The compressive elastic modulus was calculated at the five testing locations using the equation proposed earlier in the literature (Hayes et al., 1972). Since the indentation rate was generally between approximately 2 and 10 grams per second, an assumed Poisson's ratio of 0.5 was chosen to simulate an incompressible material (Mow et al., 1989).

### 2.3. μMRI protocols

μMRI experiments were carried out using a Bruker AVANCE II 300 spectrometer with a vertical-bore superconducting magnet (7T/89mm) and a micro-imaging accessory (Bruker Instrument, Billerica, MA). Using a magnetization-prepared T2 sequence (Xia, 1998), T2-weighted images were acquired at two orientations (0° and 55°, between the surface normal axis and the magnetic field direction) at the same slice location of the specimen, both before and after loading. The echo time of the contrast segment had five increments for both at 0° and 55° (Unloaded: 2, 8, 20, 40, 80 or 90 ms; Loaded: 2, 18, 40, 80, 120 or 2, 18, 40, 70, 100 ms); the echo time of the 2D mapping segment was 7.2 msec. T2 was calculated pixel–

Author Manuscript Author Manuscript Author Manuscript Author Manuscript

by-pixel by a custom routine using a single exponential fitting in MatLab (the MathWorks, Natick, MA). FOV was 4.5 mm; matrix size was 256×128; slice thickness was 0.8 mm; transverse resolution was 17.6 μm.

### 2.4. Statistical Analyses

Four sub-tissue zones were defined along the depth of cartilage: SZ, TZ, the upper radial zone (RZ1) and the lower radial zone (RZ2) (Lee et al., 2014a; Lee and Xia, 2013; Xia et al., 2001). T2 values were averaged in all sub-tissue zones, as well as over the entire tissue as the bulk. If the shape of T2(0°) profile did not resemble a typical bell-shape, the zones were divided using the averaged relative zonal thickness at each location from the bell-shape T2(0°) profiles from a related study (Lee et al., 2014b). The strain level was determined by the difference between unloaded and loaded total thickness. Only paired data from the same specimen that was imaged twice, once loaded and once unloaded, were analyzed. To determine the modifications to the topographical and zonal variations due to the external loading, (1) a student t-test was performed between each parameter before and after loading at each OA-time-point (paired) and (2) differences of each parameter before and after loading between 8X vs 8C, 12X vs 12C, and 8X vs 12X; and (3) one way ANOVA test with Bonferroni was performed for differences of each parameter among N vs 8X vs 12X. A p-value of less than 0.05 was considered an indication of statistical significance. The difference of T2 values due to loading was normalized. Using the linear regression correlation method, the normalized strain-dependent T2 was plotted as a function of the strain; and the slopes and correlation r-values were measured. The slopes were compared to determine the topographical variations of the zonal properties of cartilage while it was being loaded.

## 3. Results

### 3.1. Morphological Observations

Fig 1 showed a set of the T2 images from an 8-week OA (8X) specimen, a 12-week OA (12X) specimen, and a normal (N) specimen (Lee et al., 2014a) at 0° and 55° both before (a, b) and after (c, d) loading. At 0°, most specimens had a typical laminar appearance of cartilage, regardless of loaded or not. At the magic angle (55°), which minimizes the dipolar interaction to spin relaxation, all unloaded cartilage (8C, 12C and most of 8X and 12X) had homogeneous appearance that was similar to the normal cartilage, while some 8X and 12X cartilage surface appeared fibrillated.

### 3.2. The Depth-dependent Profiles of Cartilage With and Without Loading

Fig 2 shows a representative set of the T2 profiles at 0° (a) and 55° (b), from the same specimen (an 8X specimen) at both unloaded and loaded (L) states. All T2(0°) profiles of N, 8C, 12C specimens and most T2(0°) profiles of the 8X specimens had the bell-shape curve; in contrast, many T2(0°) profiles of the 12X specimens lost the shape (i.e., the initial dip in T2 profile), indicating surface fibrillation. When the OA progressed from normal to 12X, the values of T2 at both 0° and 55° increased. The values of loaded T2 at both 0° and 55° decreased significantly (relative to the unload tissue), more reduction near the cartilage

Author Manuscript Author Manuscript Author Manuscript Author Manuscript

surface than those near the bone interface. In addition, the depth of the peak location of the highest T2 value in the 0° profiles increased towards the deep tissue with loading.

### 3.3. Averaged Strain Dependencies of the Zonal Properties of Cartilage

The zonal averaged T2s from the meniscus-covered 8X specimens were compared in Fig 3, between the paired unloaded and loaded tissues. A gentler slope in these plots means that T2 reduces more when the tissue is compressed (i.e., the tissue is easier to be deformed by the strain). Several trends can be recognized. (1) The slopes of the linear fit were less than 1 at all zones and bulk for both 0° and 55°, indicating a reduced T2 when the tissue is compressed. (2) The largest reduction of T2 was in the surface tissue, consistent with the fact that surface tissue is softer than the deep tissue. (3) The least reduction of T2 is in the deepest tissue (RZ2), clustered nearly perfectly around the slope = 1 line, indicating little reduction upon the amount of compression. (4) The bulk values, being averaged over the entire profiles, clustered and spread closer to the diagonal line, (T2 at 0° having a slope=0.94 while T2 at 55° having a slope=0.83). Table 1 summarizes the zonal properties of articular cartilage at all topographical locations, the average strain values for the tissue blocks, and the averaged bulk moduli values for the whole medial tibia. General conclusions with regarding to the average changes of the zonal properties of the tissue as the function of the strain can be identified. (1) Zonal T2 values: T2(0°) in all zones as well as bulk decreased when loaded; T2(55°) values in all zones as well as the bulk decreased significantly except TZ ($p=0.147$), RZ1 ($p=0.347$), and RZ2 ($p=0.734$) of 12C and RZ2 (0.324) of 12X. These trends can be better understood when referring to Fig 2, which showed a distinct difference in the lower half of the tissue between 0° and 55° orientations. (2) Thickness: both SZ and TZ increased while both RZ1 and RZ2 decreased when loaded, in both absolute thickness and relative thickness at all OA-time-points. The relative thickness of SZ and TZ increased significantly except 12X ($p=0.075$) and those of RZ1 and RZ2 significantly decreased at all OA time points. These changes were due to the non-linear compression of the depth-dependent collagen matrix. (3) Modulus: both 8X and 12X had lower modulus than their contralateral specimens. Interestingly, the modulus of both groups of contralateral specimens had larger standard deviations than their OA groups, indicating more heterogeneous stiffness in the contralateral tibias.

### 3.4. Topographical Variations of the Strain Dependencies of the Zonal Properties of Cartilage

Fig 4 showed the differences of the zonal T2 due to the tissue loading as the function of OA progression, in the meniscus-covered and uncovered areas at both orientations. T2 differences were significantly increased with OA in SZ for both the covered and uncovered areas. Between 8X and 12X, T2 differences due to the tissue loading showed significantly different while those between Contralateral and OA were not significantly different. At each OA time-point, the differences of T2(0°) were the largest in the surface tissue (SZ) and smallest in the deepest tissue (RZ2), which agrees with the non-linear trend of the mechanical modulus in articular cartilage. Fig 5 shows the linear regression correlation plots, for zonal T2 ratios as the function of strain. Each regression plot contains approximately two segments: a sloped segment (0–30%) and a nearly constant segment (over 30%). All slopes in the sloped segments were measured from the fitted lines; their

Author Manuscript Author Manuscript Author Manuscript Author Manuscript

values and the correlation r-values were summarized in Table 2. Several features can be identified from the correlation analyses. (1) T2: The trends of T2 reduction due to the external loading were consistent for all OA-time-points at both 0° and 55°, which were also consistent with the normal tissue (Lee et al., 2014a). The T2 values reduced in the bulk and in nearly all zones except RZ2 of 8C. For T2(0°), the covered area had steeper slopes when compared to the uncovered area at all OA-time-points except the bulk of 8X. For bulk T2(55°), the covered area had gentler slopes when compared to the uncovered area at all OA-time-point except 12C. (2) The relative thickness: All SZ and TZ have the positive slopes while all RZ1 and RZ2 have the negative slopes, which confirmed the understanding of the zonal change in cartilage under loading. The differences of the slopes between the covered and uncovered areas of all OA tissues were smaller than those of the contralateral tissues.

Fig 6 visually summarizes the bulk values of T2(0°) slopes in Table 2 and the mechanical modulus of the specimens from Table 1. The distribution of the slopes can be divided into three groups. Group A only contains the covered areas in both contralateral tissues as well as the healthy tissue, which are well separated from the other two groups of specimens and show that the same amount of T2 changes occur at much higher modulus. In contrast, the uncovered areas in both contralateral and healthy tissues (group B) have lower modulus. The same is true for both covered and uncovered areas of the OA specimens (group C, having 8X and 12X specimens), which also had lower modulus when compared to the healthy tissue. There was no significant difference between the covered and uncovered areas in the OA tissues.

## 4. Discussion

Load bearing ability of articular cartilage is the primary function of the tissue in the organ (joint), which is weakened by OA progression. A simple external loading of cartilage would lead to both strain- and depth-dependent modification of many molecular concentrations, structures, and interactions in the extracellular matrix of the tissue (Buckwalter and Lane, 1997), caused primarily by the deformation of the collagen structure and the loss of water and ions from the tissue. While the effects of loading on bulk measures of cartilage with OA have been studied, the effect of loading on the zonal properties in cartilage with OA is largely absent (Herberhold et al., 1998; Mizrahi et al., 1986; Nag et al., 2004; Xia et al., 2011), due to the requirement of high resolution in non-destructive imaging. In a previous study of healthy cartilage, SZ of the tissue would found to deform greatly and with minimal resistance compared to RZ of the same tissue (Lee et al., 2014a), due to the depth-dependent mechanical modulus of articular cartilage. This study aimed to characterize the strain-dependent zonal properties of the medial tibial cartilage at different stages of early OA in the ACL surgery model, which is likely to cause topographically distributed damage to the surface tissue.

### 4.1. Strain dependencies of the relative thickness in OA tissue

The trends of the thickness changes of the OA tissue at most OA-time-points were found to be similar to the trends of the normal tissue (Lee et al., 2014a), that is, the relative thicknesses of the surface cartilage (SZ, TZ) increased when the tissue was loaded, and the

Author Manuscript Author Manuscript Author Manuscript Author Manuscript

relative thicknesses of the deep cartilage (RZ1, RZ2) decreased due to loading. These changes reflected the fact that the collagen fibers in the upper part of the radial zone (just under TZ) were flattened under compression and hence increased the portion of the tissue that contained the horizontal fibers, which compensated the reduction of the original surface tissue (Alhadlaq and Xia, 2004, 2005). This resulted in the reduction of the absolute thickness of the two radial zones. Topographically, the relative thicknesses of SZ and TZ cartilage in the uncovered area were also found to increase more than the covered area in the 8-week group (8X); however, the trend was reversed at 12-weeks OA specimens (12X). In most cases, the differences of the slope of relative thickness between the uncovered and covered areas decreased with OA (except TZ of 8X). These topographical variations of the depth-dependent deformations in OA cartilage have been observed in previous studies (Alhadlaq et al., 2004; Mow and Guo, 2002), where the bulk compression caused different strains at different tissue depths. Since a steeper slope can be interpreted as the tissue being more deformable with strain, our results indicated that (1) the collagen matrix of SZ was more deformable in the uncovered area than the covered area when the tissue was healthy, and (2) the difference in the resistance to deformation became smaller between the covered and uncovered areas with OA progression. These two experimental observations could be interpreted collectively as the following. When cartilage is healthy or in early OA, there are differences in cartilage deformability between the uncovered and covered areas on tibia (since not all tibial locations have the same compressive modulus). The progression of OA degrades the tissue, which will cause more damage to the harder part of the tibial surface. Consequently, the differences in the resistance to deformation would become smaller between the covered and uncovered areas with OA progression.

### 4.2. Strain dependencies of T2 in OA tissue

T2 relaxation reflects the mobility of protons in the water molecules of the tissue, modulated by the interactions between water and macromolecules, mainly the orientation and packing of the collagen fibers in the tissue. Early OA cartilage is known to have decreased proteoglycan contents, deteriorated collagen network, and increased water contents. All these degradation events will increase the mobility of water in OA tissue, which can be detected by the elevate T2 values in OA cartilage. An external loading on cartilage would cause the tissue to lose its water (and ions), modify its collagen orientation, increase the solid concentrations and increase the molecular interactions between water and macromolecules. All these loading events will reduce the mobility of water in OA tissue, which causes the reduction of T2 values in cartilage. Consequently, the influences of an external loading to OA cartilage will have competing effects to T2.

Due to the minimization of the dipolar interaction, the T2(55°) profiles are more homogeneous (c.f., Fig 2) and response more uniformly to loading compared to the T2(0°) profiles. Indeed, the slopes of the T2(55°) measurements are universally negative for all tissues in both 8-week and 12-week groups (except RZ2 at 12C). In contrast, the slopes of the T2(0°) measurements contain more complex trends, which are further influenced differently by the degeneration of cartilage. When averaged together, the slopes of the bulk T2 at the magic angle were steeper than those of 0° at 8 weeks, which was the same as in the normal tissue (Lee et al., 2014a). This consistent trend from the healthy to 8-week post

Author Manuscript Author Manuscript Author Manuscript Author Manuscript

surgery suggests that the highest sensitivity of T2 to loading occurs when the tissue is oriented at the magic angle, when the nuclear dipolar interaction in cartilage is minimized. When the tissue is oriented at 0°, the nuclear dipolar interaction has the strongest influence to spin relaxation, which could overshadow any small T2 change due to loading and OA. In contrast, at 12-week OA, the slopes at 0° were steeper than those at the magic angle, which suggests that the sensitivity of T2 to loading can be changed in OA development, likely due to the deformation of the collagen fibril network in the diseased tissue. In addition, the superficial and transitional zones have the largest changes due to loading at all OA-time-points, which reflects again the depth-dependent mechanical modulus of the tissue. These load-induced trends of T2 relaxation and relative thickness could be used in both clinical diagnostics to detect the tissue softening due to lesions and mechanical testing to measure the tissue stiffness.

### 4.3. Experimental limitations and assumptions

Several limitations and assumptions in this complex project should be considered when interpreting our results. First, we used the averaged relative zonal thickness data from the typical bell-shaped T2(0°) at each OA time point, when a T2(0°) profile lost this bell-shaped curve (due to the disruption of collagen fibril network), since any disruption should still be at the early stages and hence the zonal proportions like to change little. Second, the loading of the cartilage specimen in our μMRI experiments was done manually. To compare the profiles and values of different samples, which would be under different strains, we plotted the T2 data from various strains as the rates of the T2 changes vs. strains (Fig 5); then we fitted a slope to the changes that is strain independent. Third, the loading rate of the bulk mechanical experiment (EnduraTec instrument) did not stay constant for each test because displacement of the indenter was manually controlled. Therefore, a mean load rate was calculated through regression line fitting of a stress-strain curve to account for this factor. Fourth, the μMRI experiments were carried out with the specimens in saline with Gd contrast agent. This was done to save the total experimental time, so that we could complete all experiments for all specimens harvested from the same set of joints in a few days. (We do not use frozen samples in this project.) This approach became possible because the presence of gadolinium will reduce the value of T2 by ~10% (Nieminen et al., 2004). Since we are comparing the T2 values between OA vs contralateral tissues by the same approach, our comparison in this project is valid. Finally, the experiments were performed on 7T magnet at room temperature, which are somewhat different from clinical MRI (1.5~3T at body temperature). However, μMRI is a perfect tool for a functional study of articular cartilage due to its ability to resolve fine tissue structures and its sensitivities to the molecular environment. The “scaling law” in cartilage imaging (Xia, 2007) could lead future developments of useful procedures from microscopic to clinical resolutions, allowing successful diagnosis and management of cartilage lesion in human with mechanically induced joint diseases and injuries.

## 5. Conclusions

This study provides the direct evidence that the trends of the T2 changes in articular cartilage can be modified with the compression of cartilage. The magnitude of these changes

Author Manuscript Author Manuscript Author Manuscript Author Manuscript

was found to be highly dependent on the sub-tissue zone and amount of strain, where the larger changes occurred in SZ and TZ as compared to the deep tissue or the bulk value (similar to the low resolution imaging). Topographically, as OA progresses, the differences between the meniscus-covered and uncovered areas become smaller as the function of loading. This study demonstrates that the consequences of mechanical compression to articular cartilage can be measured by using the change of T2 in all sub-tissue zones by MRI. Since cartilage is a load-bearing tissue, monitoring the response of tissue characteristics as the function of strain serves as the functional study of cartilage and joint. This detailed knowledge of the topographical mapping and the strain-modified cartilage properties by the non-destructive MRI would be beneficial for the diagnosis and possible future treatment of OA.

## Acknowledgments

Yang Xia is grateful to the National Institutes of Health for the R01 grant (AR 052353). The authors thank Dr. Cliff Les (Henry Ford Hospital, Detroit) for constructive comments and suggestions, Dr. Nian Wang (current address: Duke University, Durham, NC) for technical help, Ms. Janelle Spann (Michigan Resonance Imaging, Rochester Hills, MI) for providing the contrast agent, and Ms. Carol Searight (Department of Physics, Oakland University) for editorial comments on the manuscript.

Funding statement: This work was supported by the National Institutes of Health [AR 052353].

Grant Support: NIH R01 grant (AR 052353)

## References

Alhadlaq HA, Xia Y. The structural adaptations in compressed articular cartilage by microscopic MRI (microMRI) T(2) anisotropy. Osteoarthritis Cartilage. 2004; 12:887–894. [PubMed: 15501404]

Alhadlaq HA, Xia Y. Modifications of orientational dependence of microscopic magnetic resonance imaging T(2) anisotropy in compressed articular cartilage. J Magn Reson Imaging. 2005; 22:665–673. [PubMed: 16220547]

Alhadlaq HA, Xia Y, Hansen FM, Les CM, Lust G. Morphological changes in articular cartilage due to static compression: polarized light microscopy study. Connect Tissue Res. 2007; 48:76–84. [PubMed: 17453909]

Alhadlaq HA, Xia Y, Moody JB, Matyas JR. Detecting structural changes in early experimental osteoarthritis of tibial cartilage by microscopic magnetic resonance imaging and polarised light microscopy. Ann Rheum Dis. 2004; 63:709–717. [PubMed: 15140779]

Brama PA, Holopainen J, van Weeren PR, Firth EC, Helminen HJ, Hyttinen MM. Effect of loading on the organization of the collagen fibril network in juvenile equine articular cartilage. J Orthop Res. 2009a; 27:1226–1234. [PubMed: 19242977]

Brama PA, Holopainen J, van Weeren PR, Firth EC, Helminen HJ, Hyttinen MM. Influence of exercise and joint topography on depth-related spatial distribution of proteoglycan and collagen content in immature equine articular cartilage. Equine Vet J. 2009b; 41:557–563. [PubMed: 19803051]

Buckwalter JA, Lane NE. Athletics and osteoarthritis. Am J Sports Med. 1997; 25:873–881. [PubMed: 9397280]

Chen SS, Falcovitz YH, Schneiderman R, Maroudas A, Sah RL. Depth-dependent compressive properties of normal aged human femoral head articular cartilage: relationship to fixed charge density. Osteoarthritis Cartilage. 2001; 9:561–569. [PubMed: 11520170]

Dunn TC, Lu Y, Jin H, Ries MD, Majumdar S. T2 relaxation time of cartilage at MR imaging: comparison with severity of knee osteoarthritis. Radiology. 2004; 232:592–598. [PubMed: 15215540]

Author Manuscript Author Manuscript Author Manuscript Author Manuscript

Eckstein F, Faber S, Muhlbauer R, Hohe J, Englmeier KH, Reiser M, Putz R. Functional adaptation of human joints to mechanical stimuli. Osteoarthritis Cartilage. 2002; 10:44–50. [PubMed: 11795982]

Fragonas E, Mlynarik V, Jellus V, Micali F, Piras A, Toffanin R, Rizzo R, Vittur F. Correlation between biochemical composition and magnetic resonance appearance of articular cartilage. Osteoarthritis Cartilage. 1998; 6:24–32. [PubMed: 9616436]

Hayes WC, Keer LM, Herrmann G, Mockros LF. A mathematical analysis for indentation tests of articular cartilage. J Biomech. 1972; 5:541–551. [PubMed: 4667277]

Herberhold C, Stammberger T, Faber S, Putz R, Englmeier KH, Reiser M, Eckstein F. An MR-based technique for quantifying the deformation of articular cartilage during mechanical loading in an intact cadaver joint. Magn Reson Med. 1998; 39:843–850. [PubMed: 9581616]

Jones EF, Schooler J, Miller DC, Drake CR, Wahnishe H, Siddiqui S, Li X, Majumdar S. Characterization of Human Osteoarthritic Cartilage Using Optical and Magnetic Resonance Imaging. Mol Imaging Biol. 2012; 14:32–39. [PubMed: 21384207]

Jurvelin JS, Arokoski JP, Hunziker EB, Helminen HJ. Topographical variation of the elastic properties of articular cartilage in the canine knee. J Biomech. 2000; 33:669–675. [PubMed: 10807987]

Lee JH, Badar F, Kahn D, Matyas J, Qu X, Chen CT, Xia Y. Topographical Variations of the Strain-dependent Zonal Properties of Tibial Articular Cartilage by Microscopic MRI. Connect Tissue Res. 2014a; 55:205–216. [PubMed: 24559385]

Lee, JH.; Badar, F.; Matyas, J.; Xia, Y. the 60th Orthopaedic Research Society (ORS). 2014b. Topographic Modifications of T2 and Cartilage Thickness in the Early Stages of Experimental Osteoarthritis in Canine Tibial Cartilage by Magnetic Resonance Imaging Methods at Microscopic Resolution.

Lee JH, Xia Y. Quantitative zonal differentiation of articular cartilage by microscopic magnetic resonance imaging, polarized light microscopy, and Fourier-transform infrared imaging. Microscopy research and technique Microsc Res Tech 2013. 2013 Jun; 76(6):625–32.

Mizrahi J, Maroudas A, Lanir Y, Ziv I, Webber TJ. The “instantaneous” deformation of cartilage: effects of collagen fiber orientation and osmotic stress. Biorheology. 1986; 23:311–330. [PubMed: 3779058]

Mow VC, Gibbs MC, Lai WM, Zhu WB, Athanasiou KA. Biphasic indentation of articular cartilage--II. A numerical algorithm and an experimental study. J Biomech. 1989; 22:853–861. [PubMed: 2613721]

Mow VC, Guo XE. Mechano-electrochemical properties of articular cartilage: their inhomogeneities and anisotropies. Annu Rev Biomed Eng. 2002; 4:175–209. [PubMed: 12117756]

Murphy LST, Helmick CG, Renner JB, Tudor G, Koch G, Dragomir A, Kalsbeek WD, Luta G, Jordan JM. Lifetime risk of symptomatic knee osteoarthritis. Arthritis and rheumatism. 2008; 59:1207–1213. [PubMed: 18759314]

Nag D, Liney GP, Gillespie P, Sherman KP. Quantification of T(2) relaxation changes in articular cartilage with in situ mechanical loading of the knee. J Magn Reson Imaging. 2004; 19:317–322. [PubMed: 14994300]

Nieminen MT, Menezes NM, Williams A, Burstein D. T2 of articular cartilage in the presence of Gd-DTPA2. Magn Reson Med. 2004; 51:1147–1152. [PubMed: 15170834]

Nissi MJ, Rieppo J, Toyras J, Laasanen MS, Kiviranta I, Nieminen MT, Jurvelin JS. Estimation of mechanical properties of articular cartilage with MRI - dGEMRIC, T2 and T1 imaging in different species with variable stages of maturation. Osteoarthritis Cartilage. 2007; 15:1141–1148. [PubMed: 17513137]

Stahl R, Blumenkrantz G, Carballido-Gamio J, Zhao S, Munoz T, Hellio Le Graverand-Gastineau MP, Li X, Majumdar S, Link TM. MRI-derived T2 relaxation times and cartilage morphometry of the tibio-femoral joint in subjects with and without osteoarthritis during a 1-year follow-up. Osteoarthritis Cartilage. 2007; 15:1225–1234. [PubMed: 17561417]

Wayne JS, Kraft KA, Shields KJ, Yin C, Owen JR, Disler DG. MR imaging of normal and matrix-depleted cartilage: correlation with biomechanical function and biochemical composition. Radiology. 2003; 228:493–499. [PubMed: 12893905]

Author Manuscript Author Manuscript Author Manuscript Author Manuscript

Weiss C, Rosenberg L, Helfet AJ. An ultrastructural study of normal young adult human articular cartilage. J Bone Joint Surg Am. 1968; 50:663–674. [PubMed: 5658553]

Xia Y. Relaxation anisotropy in cartilage by NMR microscopy (μMRI) at 14-microm resolution. Magn Reson Med. 1998; 39:941–949. [PubMed: 9621918]

Xia Y. Heterogeneity of cartilage laminae in MR imaging. J Magn Reson Imaging. 2000; 11:686–693. [PubMed: 10862069]

Xia Y. Resolution 'scaling law' in MRI of articular cartilage. Osteoarthritis Cartilage. 2007; 15:363–365. [PubMed: 17218119]

Xia Y, Alhadlaq H, Ramakrishnan N, Bidthanapally A, Badar F, Lu M. Molecular and morphological adaptations in compressed articular cartilage by polarized light microscopy and Fourier-transform infrared imaging. J Struct Biol. 2008; 164:88–95. [PubMed: 18634884]

Xia Y, Elder K. Quantification of the graphical details of collagen fibrils in transmission electron micrographs. J Microsc. 2001; 204:3–16. [PubMed: 11580808]

Xia Y, Moody JB, Alhadlaq H, Hu J. Imaging the physical and morphological properties of a multi-zone young articular cartilage at microscopic resolution. J Magn Reson Imaging. 2003; 17:365–374. [PubMed: 12594728]

Xia Y, Moody JB, Burton-Wurster N, Lust G. Quantitative in situ correlation between microscopic MRI and polarized light microscopy studies of articular cartilage. Osteoarthritis Cartilage. 2001; 9:393–406. [PubMed: 11467887]

Xia Y, Wang N, Lee J, Badar F. Strain-dependent T1 relaxation profiles in articular cartilage by MRI at microscopic resolutions. Magn Reson Med. 2011; 65:1733–1737. [PubMed: 21452280]

Author Manuscript Author Manuscript Author Manuscript Author Manuscript

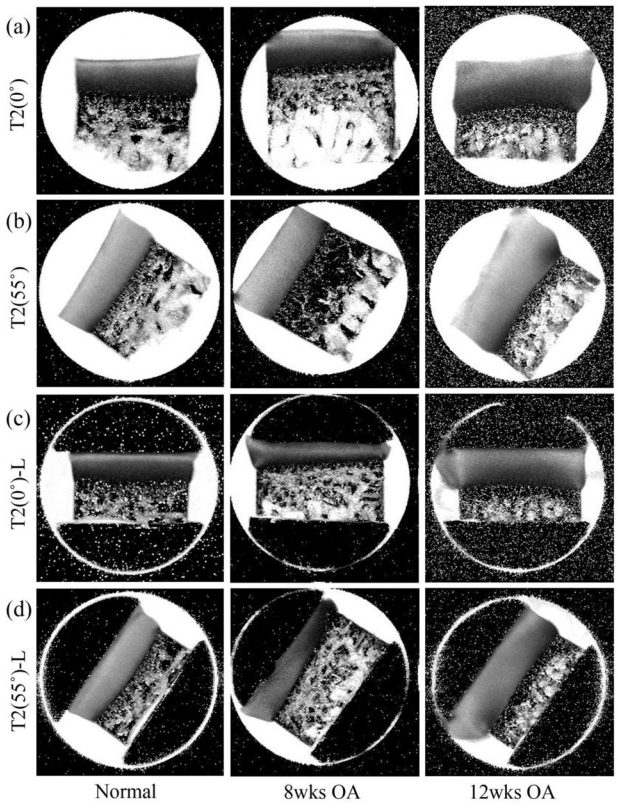


**Figure 1.**

A representative set of the quantitative MRI T2 images at two orientations (0° and 55°) in the magnetic field $B_0$ (pointed upward), from three specimens (Normal-N, 8wk OA-8X, 12wk OA-12X) without loading (a, b) and being loaded (c, d). The display intensities of all images in the figure are 0 to 100.

Author Manuscript Author Manuscript Author Manuscript Author Manuscript

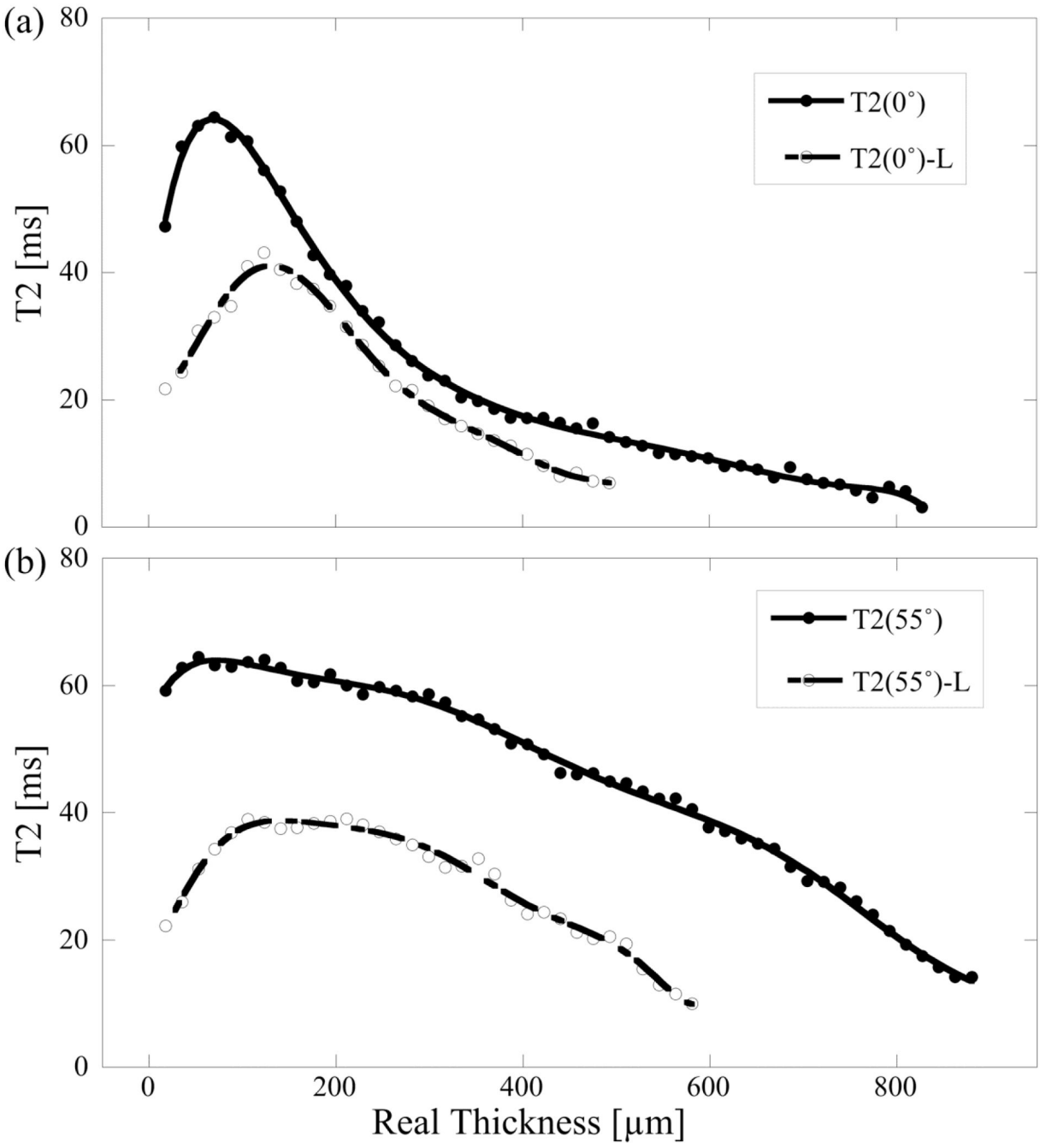


**Figure 2.**
A representative set of the depth dependent T2 profiles at 0° (a) and 55° (b), before and after loading (L) at ~30% strain.

Author Manuscript Author Manuscript Author Manuscript Author Manuscript

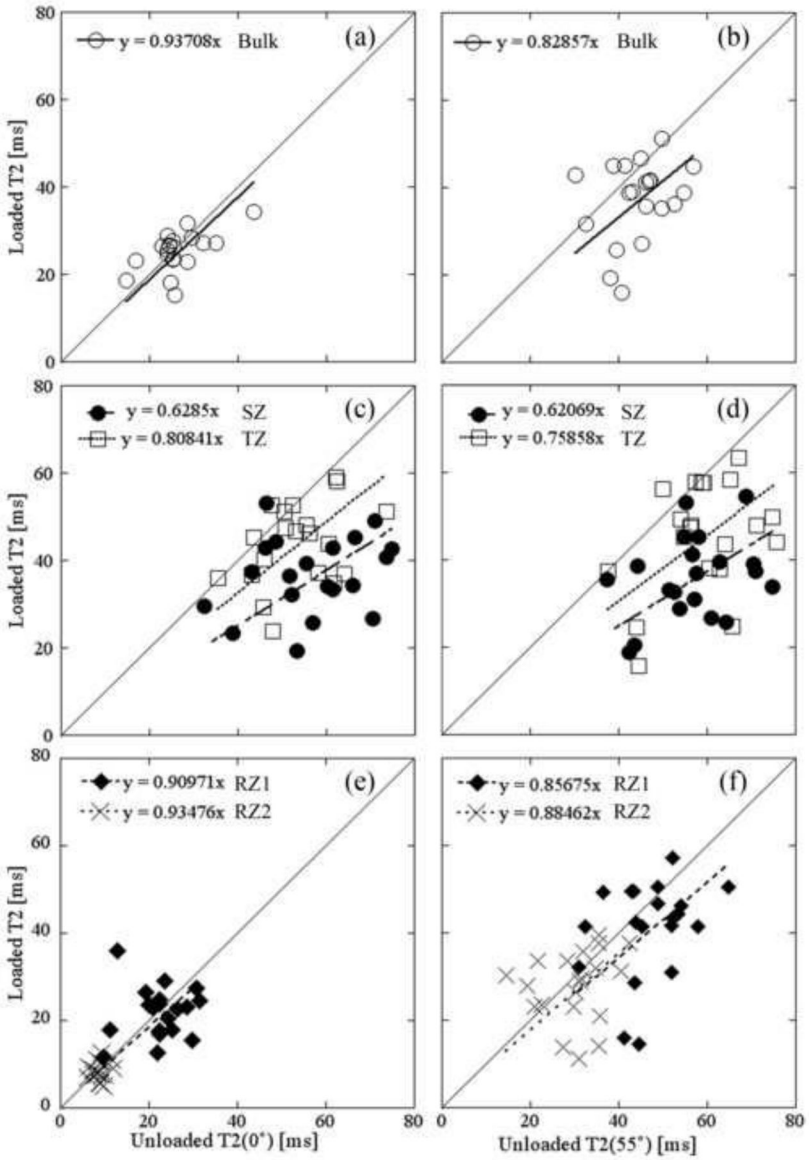


**Figure 3.**

A representative set of the paired and averaged T2 data at 0° (left) and 55° (right) before and after loading with linear regression in bulk (a, b), SZ and TZ (c, d), and RZ1 and RZ2 (e, f) from the meniscus-covered regions of 8X specimens. Each data point represents the averaged zonal T2 value both before (horizontal) and after loading (vertical) of the same specimen. The solid line has a slope of 1. The slopes of linear fit less than one indicates the T2 values decreased with loading.

Author Manuscript Author Manuscript Author Manuscript Author Manuscript

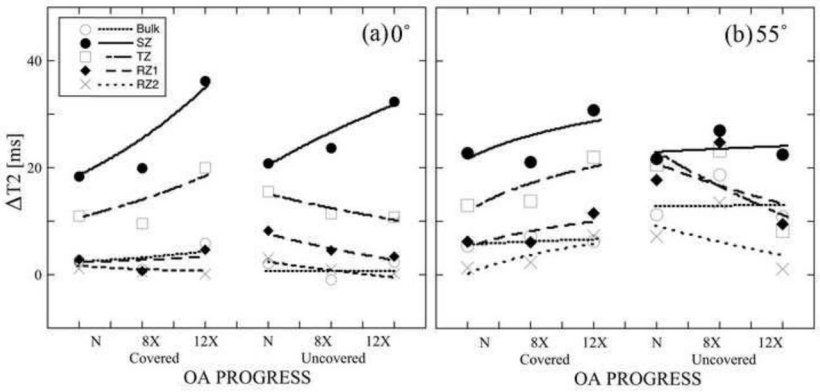


**Figure 4.**

Average zonal differences of T2 before and after loading at each OA-time-point for both the meniscus-covered and uncovered areas at 0° (a) and at 55° (b).

Author Manuscript Author Manuscript Author Manuscript Author Manuscript

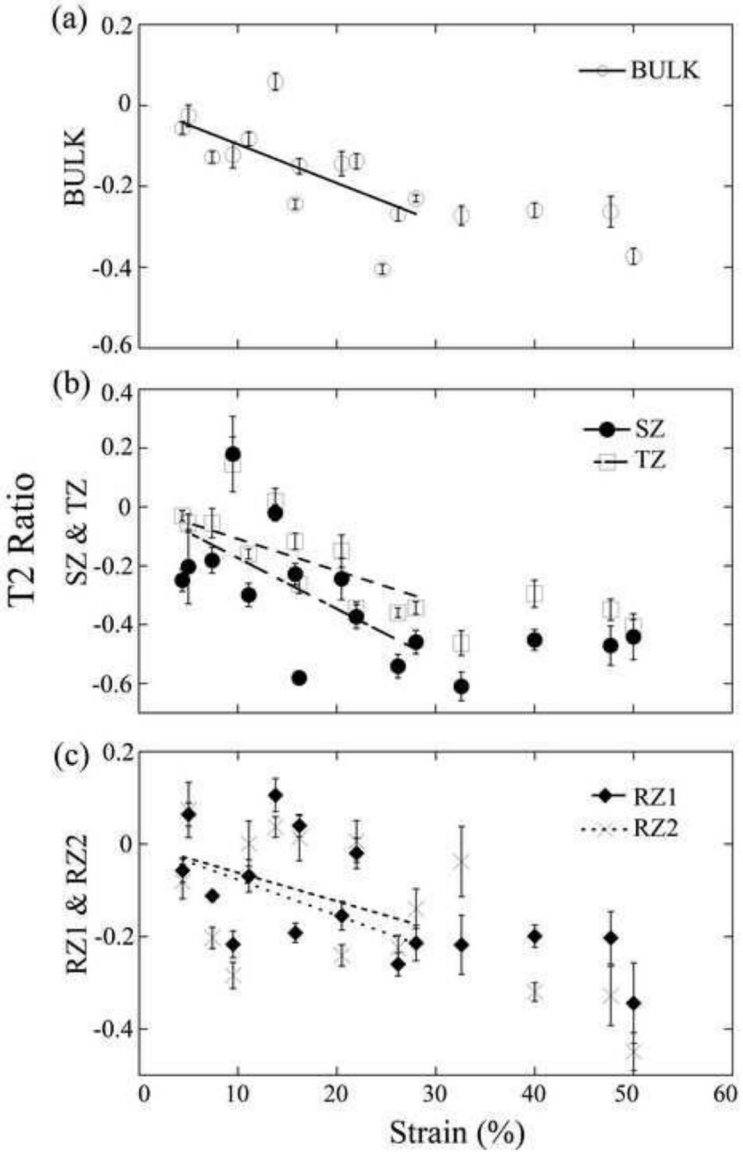


**Figure 5.**

A representative set of the load-induced changes of T2 ratio of the bulk (a), the SZ and TZ (b), and the RZ1 and RZ2 (c) in the meniscus-covered area at 8-weeks contralateral. Each dot represents 10 averaged T2 values.

Author Manuscript Author Manuscript Author Manuscript Author Manuscript

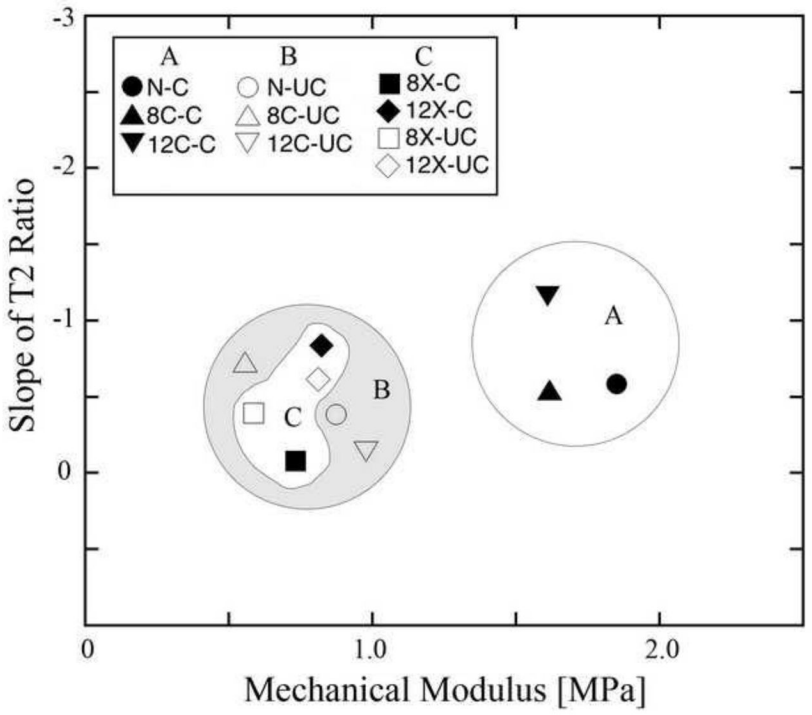


**Figure 6.**

The distributions of the slopes of the load-induced changes of bulk T2(0°) ratio of at each OA-time-point versus mechanical modulus. Solid color represents the meniscus-covered area and the empty ones represent the uncovered area.

Author Manuscript Author Manuscript Author Manuscript Author Manuscript





**Table 1**

Mean ± standard deviation (SD) within each sub-tissue zone for all measurements from medial tibia cartilage specimens at each OA-time-point with and without loading

| Sub-tissue Zone | 8wk-Contralateral | | 8wk-OA | | 12wk-Contralateral | | 12wk-OA | |
|---|---|---|---|---|---|---|---|---|
| | Mean | SD | Mean | SD | Mean | SD | Mean | SD |
| T2(0°)-Unloaded [ms] | | | | | | | | |
| Bulk | 26.0 | 7.1 | 26.4 | 6.0 | 31.1 | 9.1 | 29.7 | 6.6 |
| SZ | 53.6 | 15.1 | 59.1 | 12.9 | 58.3 | 20.7 | 66.2 | 17.4 |
| TZ | 54.9 | 13.1 | 56.7 | 11.4 | 64.5 | 18.8 | 63.9 | 17.6 |
| RZ1 | 23.3 | 8.1 | 24.4 | 7.2 | 30.5 | 9.5 | 27.7 | 6.5 |
| RZ2 | 9.9 | 2.8 | 9.6 | 2.0 | 13.4 | 4.1 | 11.6 | 2.2 |
| T2(0°)-Loaded [ms] | | | | | | | | |
| Bulk | 25.7 *c* | 7.4 | 26.1 *c* | 6.2 | 24.2 *c* | 3.8 | 25.5 *b* | 4.1 |
| SZ | 36.6 *a* | 10.8 | 37.7 *a* | 9.7 | 30.5 *b* | 4.9 | 31.8 *a* | 5.7 |
| TZ | 45.3 *a* | 11.9 | 46.4 *a* | 11.1 | 43.1 *b* | 5.3 | 48.1 *b* | 12.1 |
| RZ1 | 22.3 *c* | 10.1 | 22.1 *b* | 7.2 | 21.8 *b* | 4.3 | 23.6 *b* | 4.6 |
| RZ2 | 9.6 *c* | 3.9 | 8.9 *c* | 2.6 | 11.2 *b* | 2.2 | 11.5 *c* | 3.5 |
| T2(55°)-Unloaded [ms] | | | | | | | | |
| Bulk | 45.4 | 10.4 | 49.2 | 8.8 | 46.7 | 12.3 | 48.2 | 10.8 |
| SZ | 56.6 | 13.7 | 58.9 | 11.3 | 49.3 | 18.1 | 63.2 | 12.3 |
| TZ | 58.6 | 13.7 | 62.8 | 11.5 | 55.4 | 20.6 | 64.9 | 11.7 |
| RZ1 | 50.0 | 13.1 | 54.6 | 12.6 | 53.3 | 20.4 | 56.0 | 16.5 |
| RZ2 | 32.6 | 9.7 | 34.7 | 8.6 | 36.5 | 12.4 | 35.6 | 8.0 |
| T2(55°)-Loaded [ms] | | | | | | | | |
| Bulk | 36.7 | 10.3 | 37.5 *a* | 9.3 | 39.0 *a* | 9.7 | 40.0 *a* | 7.8 |
| SZ | 37.5 *a* | 12.0 | 35.5 *a* | 9.9 | 30.8 *b* | 5.2 | 37.0 *b* | 9.3 |
| TZ | 44.7 *a* | 11.9 | 45.4 *a* | 11.9 | 46.3 *c* | 9.3 | 50.6 *b* | 13.5 |
| RZ1 | 39.8 *a* | 13.9 | 41.1 *a* | 11.9 | 49.0 *c* | 15.5 | 45.6 *b* | 15.0 |
| RZ2 | 26.8 *b* | 9.2 | 28.0 *a* | 8.4 | 35.6 *c* | 11.1 | 31.7 *c* | 11.3 |
| Real Thickness-Unloaded [μm] | | | | | | | | |

Author Manuscript Author Manuscript Author Manuscript Author Manuscript



| Sub-tissue Zone | 8wk-Contralateral | | 8wk-OA | | 12wk-Contralateral | | 12wk-OA | |
|---|---|---|---|---|---|---|---|---|
| | Mean | SD | Mean | SD | Mean | SD | Mean | SD |
| Bulk | 1062.8 | 301.9 | 1133.4 | 367.0 | 1148.7 | 337.9 | 1152.5 | 321.0 |
| SZ | 40.5 | 13.2 | 43.7 | 22.9 | 33.7 | 14.0 | 28.4 | 11.4 |
| TZ | 150.8 | 34.5 | 152.0 | 44.2 | 161.3 | 45.5 | 157.0 | 42.8 |
| RZ1 | 438.2 | 145.2 | 468.8 | 172.2 | 456.1 | 121.8 | 449.5 | 116.9 |
| RZ2 | 428.9 | 144.0 | 468.4 | 172.4 | 447.3 | 123.2 | 437.3 | 117.4 |
| Real Thickness-Loaded [μm] | | | | | | | | |
| Bulk | 826.2 *a* | 322.0 | 816.0 *a* | 250.0 | 839.7 *a* | 184.0 | 867.4 *a* | 221.3 |
| SZ | 44.0 *c* | 20.0 | 44.8 *c* | 22.5 | 42.5 *b* | 14.0 | 50.1 *a* | 14.1 |
| TZ | 166.0 *c* | 52.7 | 183.5 *c* | 84.4 | 170.1 *c* | 40.6 | 155.6 *c* | 39.2 |
| RZ1 | 316.8 *a* | 145.9 | 299.2 *a* | 105.1 | 319.7 *a* | 82.2 | 326.3 *a* | 106.8 |
| RZ2 | 305.7 *a* | 143.3 | 288.5 *a* | 107.3 | 312.4 *a* | 78.8 | 320.9 *a* | 106.1 |
| Relative Thickness-Unloaded [%] | | | | | | | | |
| SZ | 4.0 | 1.4 | 4.2 | 3.0 | 3.3 | 1.8 | 3.8 | 3.8 |
| TZ | 14.9 | 3.8 | 14.5 | 5.8 | 15.5 | 6.3 | 15.1 | 4.3 |
| RZ1 | 41.0 | 2.1 | 40.7 | 3.9 | 40.9 | 3.7 | 41.6 | 2.3 |
| RZ2 | 40.1 | 2.2 | 40.6 | 4.0 | 40.2 | 4.0 | 40.5 | 2.3 |
| Relative Thickness-Loaded [%] | | | | | | | | |
| SZ | 5.9 *b* | 3.0 | 6.7 *b* | 5.7 | 5.2 *b* | 2.1 | 6.3 *c* | 2.6 |
| TZ | 21.0 *a* | 5.7 | 22.9 *a* | 6.3 | 20.9 *b* | 6.7 | 19.4 *b* | 6.5 |
| RZ1 | 37.5 *a* | 3.8 | 36.2 *a* | 4.9 | 37.4 *b* | 4.0 | 37.5 *b* | 4.4 |
| RZ2 | 35.9 *a* | 3.4 | 34.7 *a* | 5.2 | 36.5 *b* | 3.7 | 36.8 *b* | 4.3 |
| Strain [%] | | | | | | | | |
| Bulk | 23.2 | 13.8 | 26.4 | 13.5 | 25.8 | 13.7 | 27.0 | 10.5 |
| Zone | 23.2 | 13.8 | 26.4 | 13.5 | 19.6 | 9.5 | 24.6 | 13.8 |

The statistical results of the paired student t-test between unloaded and loaded on parameters were shown by the superscript letter:

*a* P<0.001,

*b* p<0.05,

*c* p>0.05

Author Manuscript Author Manuscript Author Manuscript Author Manuscript





*J Biomech*. Author manuscript; available in PMC 2016 October 15.

**Table 2**

The slopes of the Ratio $((V_L - V_{UL})/V_{UL})$ vs. strains with correlation r-values at the meniscus-covered and uncovered areas

| Sub-tissue Zone | 8wk-Contralateral | | 8wk-OA | | 12wk-Contralateral | | 12wk-OA | |
|---|---|---|---|---|---|---|---|---|
| | **Slope** | **r-value** | **Slope** | **r-value** | **Slope** | **r-value** | **Slope** | **r-value** |
| T2(0°) Ratio vs. Strains-Covered | | | | | | | | |
| Bulk | −0.544 | 0.331 *a* | −0.081 | 0.321 *a* | −1.162 | 0.296 *b* | −0.840 | 0.103 *c* |
| SZ | −0.651 | 0.751 *a* | −1.685 | 0.654 *a* | −2.139 | 0.447 *b* | −2.960 | 0.322 *b* |
| TZ | −0.958 | 0.581 *a* | −0.745 | 0.759 *a* | −1.554 | 0.455 *a* | −1.207 | 0.032 *c* |
| RZ1 | −0.366 | 0.400 *a* | −0.433 | 0.640 *a* | −1.484 | 0.423 *b* | −0.859 | 0.523 *a* |
| RZ2 | −0.474 | 0.467 *a* | −0.229 | 0.389 *a* | −0.563 | 0.151 *c* | −0.785 | 0.369 *b* |
| T2(0°) Ratio vs. Strains -Uncovered | | | | | | | | |
| Bulk | 0.728 | 0.167 *a* | 0.392 | 0.542 *a* | −0.141 | 0.667 *a* | −0.615 | 0.291 *b* |
| SZ | −1.401 | 0.544 *a* | −1.228 | 0.804 *a* | −1.336 | 0.425 *b* | −2.435 | 0.155 *c* |
| TZ | −0.615 | 0.403 *b* | −0.528 | 0.691 *a* | −0.776 | 0.944 *a* | −0.808 | 0.100 *c* |
| RZ1 | 0.707 | 0.310 *b* | −0.294 | 0.268 *b* | −0.387 | 0.501 *a* | −0.713 | 0.136 *c* |
| RZ2 | 0.402 | 0.455 *a* | 0.042 | 0.108 *c* | 0.025 | 0.319 *b* | −0.287 | 0.237 *c* |
| T2(55°) Ratio vs. Strains -Covered | | | | | | | | |
| Bulk | −0.954 | 0.681 *a* | −0.456 | 0.356 *a* | −0.937 | 0.641 *a* | −0.341 | 0.291 *a* |
| SZ | −1.852 | 0.523 *a* | −1.656 | 0.462 *a* | −1.354 | 0.969 *a* | −2.207 | 0.923 *a* |
| TZ | −1.161 | 0.790 *a* | −0.823 | 0.555 *a* | −0.965 | 0.984 *a* | −0.978 | 0.229 *c* |
| RZ1 | −0.746 | 0.530 *a* | −0.119 | 0.250 *b* | −0.742 | 0.940 *a* | −0.534 | 0.108 *c* |
| RZ2 | −0.959 | 0.294 *a* | −0.386 | 0.043 *c* | −0.764 | 0.930 *a* | −0.004 | 0.442 *b* |
| T2(55°) Ratio vs. Strains -Uncovered | | | | | | | | |
| Bulk | −1.140 | 0.824 *a* | −1.254 | 0.820 *a* | −0.130 | 0.186 *c* | −0.488 | 0.171 *c* |
| SZ | −1.526 | 0.671 *a* | −1.554 | 0.688 *a* | −2.088 | 0.339 *b* | −1.474 | 0.124 *c* |
| TZ | −1.557 | 0.956 *a* | −1.173 | 0.694 *a* | −0.619 | 0.147 *c* | −0.307 | 0.305 *c* |
| RZ1 | −1.676 | 0.832 *a* | −1.474 | 0.789 *a* | −0.164 | 0.282 *c* | −0.476 | 0.065 *c* |
| RZ2 | −0.428 | 0.271 *b* | −1.290 | 0.734 *a* | 0.188 | 0.245 *c* | −0.025 | 0.702 *a* |

Author Manuscript Author Manuscript Author Manuscript Author Manuscript



| Sub-tissue Zone | 8wk-Contralateral | | 8wk-OA | | 12wk-Contralateral | | 12wk-OA | |
|---|---|---|---|---|---|---|---|---|
| | Slope | r-value | Slope | r-value | Slope | r-value | Slope | r-value |
| Relative Thickness Ratio vs. Strains -Covered | | | | | | | | |
| SZ | 2.714 | 0.124 *c* | 2.459 | 0.080 *c* | 1.735 | 0.384 *c* | 6.256 | −0.139 *c* |
| TZ | 1.630 | 0.675 *b* | 1.609 | 0.109 *c* | 2.463 | 0.627 *c* | 0.824 | 0.094 *c* |
| RZ1 | −0.336 | −0.586 *b* | −0.022 | 0.160 *c* | −0.545 | −0.600 *c* | −0.477 | −0.194 *c* |
| RZ2 | −0.470 | −0.508 *c* | −0.440 | −0.472 *c* | −0.466 | −0.358 *c* | −0.430 | −0.080 *c* |
| Relative Thickness Ratio vs. Strains -Uncovered | | | | | | | | |
| SZ | 3.804 | 0.837 *a* | 2.497 | 0.393 *c* | 4.386 | 0.202 *c* | 5.145 | −0.085 *c* |
| TZ | 2.319 | 0.837 *b* | 5.048 | 0.035 *c* | 1.455 | 0.043 *c* | 1.403 | 0.145 *c* |
| RZ1 | −0.494 | −0.930 *b* | −0.578 | −0.041 *c* | −0.226 | −0.323 *c* | −0.239 | −0.222 *c* |
| RZ2 | −0.524 | −0.830 *c* | −0.619 | 0.103 *c* | −0.291 | 0.100 *c* | −0.198 | −0.037 *c* |

The significances of the correlation were indicated by the superscript letter:

*a* P<0.001,

*b* p<0.05,

*c* p>0.05.